

The mechanical and tribological characteristic of Aluminium-Titanium dioxide composites

Levent Ulvi Gezici^a, Burak Gül^a, Uğur Çavdar^{b,✉}

^aCelal Bayar University, Engineering Faculty, Department of Mechanical Engineering, 45140 Manisa, Turkey
^bİzmir Demokrasi University, Engineering Faculty, Mechanical Engineering Department, İDU Campus, 35140, İzmir/Turkey
[✉]Corresponding Author: ugur.cavdar@idu.edu.tr

Submitted: 10 December 2016; Accepted: 4 December 2017; Available On-line: 29 May 2018

ABSTRACT: The purpose of this work was to investigate the mechanical and tribological effects of Titanium dioxide (TiO₂) reinforcement in Aluminium (Al). Aluminium composites consist of 99.8% pure aluminium reinforced with five different portions of TiO₂. Aluminium powders were mixed with TiO₂ by ball milling for 30 minutes in a planetary mixer. The powder mixture was compacted by the cold pressing technique at 250 MPa. Two different methods used for sintering. The green compact was sintered at 600 °C for 300 seconds in open atmosphere with an Ultra-High Frequency Induction System (UHFIS) and with furnace at 600 °C for 1800 seconds. The mechanical and microstructural properties of examples were compared for different amount of reinforcement. We have observed a maximum hardness for 5 wt.% TiO₂ reinforced composites.

KEYWORDS: Aluminium; TiO₂; Induction sintering; Powder metallurgy

Citation/Citar como: Ulvi Gezici, L.; Gül, B.; Çavdar, U. (2018). "The mechanical and tribological characteristic of Aluminium-Titanium dioxide composites". *Rev. Metal.* 54(2): e119. <https://doi.org/10.3989/revmetalm.119>

RESUMEN: *Características mecánicas y tribológicas de compuestos de dióxido de Titanio-Aluminio.* El objetivo de este trabajo es investigar las propiedades mecánicas y tribológicas de refuerzos de dióxido de titanio (TiO₂) en una matriz de aluminio (Al). Se utilizó aluminio de pureza 99,8% reforzado con TiO₂ ensayándose cinco cantidades diferentes de dióxido de titanio. Se mezcló polvo de aluminio y TiO₂ en un molino de bolas durante 30 min, utilizando un mezclador con eje descentrado. La mezcla se compactó mediante la técnica de prensado en frío a una presión de 250 MPa. Se utilizaron dos métodos diferentes para el sinterizado. El compactado en verde se sinterizó a 600 °C durante 300 s en atmósfera ambiental con un sistema de inducción de ultra alta frecuencia (UHFIS) y con un horno convencional a 600 °C durante 1800 s. Las propiedades mecánicas y microestructurales de las muestras se compararon utilizando diferentes cantidades de refuerzo. La dureza máxima se observó para un refuerzo con 5% en peso de TiO₂.

PALABRAS CLAVE: Aluminio; TiO₂; Sinterización por inducción; Metalurgia de polvos

ORCID ID: Levent Ulvi Gezici (<https://orcid.org/0000-0002-0353-3270>); Burak Gül (<https://orcid.org/0000-0002-4446-4259>); Uğur Çavdar (<https://orcid.org/0000-0002-3434-6670>)

Copyright: © 2018 CSIC. This is an open-access article distributed under the terms of the Creative Commons Attribution 4.0 International (CC BY 4.0) License.

1. INTRODUCTION

Aluminium alloys used in many applications because of their high strength, low density and good formability. The limiting factor was the poor surface hardness and wear resistance (Xiang *et al.*, 2015). Especially aluminium based metal matrix composites (MMCs) are used in manufacturing industry due to their low cost and weight (Singh *et al.*, 2015). Aluminium based MMCs have improved wears resistance, toughness and superplastic forming which make Al more attractive than other metals (Pydi *et al.*, 2013; Hassani *et al.*, 2014; Singh *et al.*, 2015). Aluminium matrix composites (AMCs) reinforced with ceramic particles are relatively easy to process which are applied in various industrial domains (Hassani *et al.*, 2014). In the straight compaction and sintering of Al powder have some complexities due to the presence of an oxide layer covering the powder particles (Gökçe and Fındık, 2008). Typically the oxide layer on bulk aluminium at room temperature varies between 10 to 20 nm while the layer can vary between 50 and 150 nm on powder. This layer acts as a barrier to solid state sintering (SSS). However additions of Mg have been shown to be effective in disrupting the oxide layer and facilitating the SSS of aluminium (Lumley, 2011).

Titanium dioxide (TiO₂) is a single crystalline system in the surface science of metal oxides. TiO₂ has three different phases in nature which are anatase, rutile and brookite. It is used as a heterogeneous catalyst and photocatalyst. It also finds applications in solar cells. TiO₂ used in gas sensors and in paint industries as white pigment (Chuang *et al.*, 2011). The surface science of TiO₂ shows a rapid growth of interest among researchers and scientists. TiO₂ film coating is used for improving corrosion resistance, mechanical properties and surface energy (Leng *et al.*, 2007; Aniolek *et al.*, 2016). In addition TiO₂ coating is used on aircraft surface since it absorbs the radar signals (Raut and Choudhary, 2015).

TiO₂ has a high diffraction index and it requires a particle size of approximately half the wavelength of the light for strong light scattering capability. There are some difficulties by working with nanoparticles. TiO₂ particles tend to agglomerate due to their large-surface area and nano size effect. Large particle sizes improve dispersion but small particle size leads to higher Van Der Waals Forces which decrease the dispersion of the particles. Only well dispersed TiO₂ nanoparticles can lead a unique properties of the composites (Pinto *et al.*, 2015).

TiO₂ particle sintering does not happen up to 1000 °C and pure anatase transformation begins into a rutile at about 600 °C in air. The transformation also depends on the heating rate (Tubio *et al.*, 2015). So the relative density and grain size of TiO₂ were usually investigated as a function of sintering

time and heating rate. At higher heating rates amorphous TiO₂ transformed to rutile directly while at a lower heating rates the amorphous transformed to anatase at 500 °C and then to rutile at 800–900 °C (Li *et al.*, 2010). The density does not change at temperatures between 650–800 °C. But at temperatures between 800–1000 °C, the grain boundary diffusion causes densification and grain growth (Mazaheri *et al.*, 2009).

The aim of this study was to examine the effect of TiO₂ reinforcement in aluminium. For this purpose the density, porosity, hardness, wear resistance, and microstructure of Al-TiO₂ composites were investigated. The green compacts with the same percent of reinforcement were sintered with induction and furnace. The results of induction and furnace sintered examples have been compared with each other to see the mechanical and tribological effects of the sinter method.

2. MATERIALS AND METHODS

By paper research we recognize that the TiO₂ reinforcement effect on mechanical properties does not change much after 10 wt.% reinforcement. And the maximum change is between 0–5 wt.% reinforcement. Therefore, we chose to study 1, 3, 5, 9 and 15 wt.% TiO₂ reinforcement rates. Aluminium based composites that consist of 99.8% pure Al was reinforced with 99.5% pure TiO₂. The size of particles was 50–70 micron for Al and 200–350 nm for TiO₂. The mixture was ball milled in a planetary ball mill with 30 steel balls at a speed of 56 rpm for 30 min for hindering agglomeration. The ball to powder mass ratio was 10:1, 15:1, 20:1. For each sample 2 gram powder was compacted at 250 MPa by cold isostatic pressing. Thirty green samples with 16 mm diameter and 4 mm thickness were pressed. Ten of them were sintered by a conventional sintering in an electric resistance Protherm furnace at 600 °C for 1800 seconds with a heating rate of 10 °C/second. Other ten samples were sintered with induction and with the same reinforcement portions at 600 °C for 300 seconds with a heating rate of 100 °C/second. The UHFIS using 2.8 kW and 900 kHz with a cylindrical coil with inner diameter of 20 mm. This system was called UHFIS by Çavdar and Gülşahin (2014) and Çavdar, P. and Çavdar, U. (2015), because of its very high frequency. Both sinter application was under an atmospheric environment.

The wear resistance of sintered Al-TiO₂ composite samples was investigated at room temperature using a CSM Tribometer with pin on disk test against a 5 mm diameter steel ball with 5 N load. The wear test performed approximately 7950 laps, 100 m way and 1000 seconds. The weight of samples was recorded before and after testing (Tables 1–3). The Brinell hardness test of sintered samples was performed using a BMS 200-RB (Rockwell & Brinell)

TABLE 1. By 250 MPa pressed and furnace sintered samples at 600 °C for 30 min

TiO ₂ wt.%	Powder	After Pressing		After Sintering		Density (g·cm ⁻³)	Hardness (HB)
	Weight (g)	Weight (g)	Volume (cm ³)	Weight (g)	Volume (cm ³)		
1	2.0027	1.9999	0.7984	2.0033	0.7923	2.6907	48
3	2.0018	1.9951	0.7994	2.0004	0.7923	2.7249	50
5	2.0009	1.9917	0.7984	1.999	0.7920	2.7558	51
9	2.0108	2.0101	0.8004	2.0163	0.7923	2.7781	48
15	2.0509	2.0038	0.8004	2.0066	0.7943	2.7297	30

^a(Error range [ER] is $\pm 2\%$).

TABLE 2. By 250 MPa pressed and induction sintered samples at 600 °C for 5 min

TiO ₂ wt.%	Powder	After Pressing		After Sintering		Density (g·cm ⁻³)	Hardness (HB)
	Weight (g)	Weight (g)	Volume (cm ³)	Weight (g)	Volume (cm ³)		
1	2.0111	2.0067	0.8004	2.0074	0.7923	2.6879	49
3	2.0174	2.0131	0.8086	2.0156	0.7923	2.6996	53
5	2.0294	2.0166	0.8014	2.0172	0.7932	2.7258	54
9	2.0144	2.0131	0.7963	2.0128	0.7943	2.6986	49
15	2.001	1.9982	0.8004	2.0174	0.7973	2.7698	34

^a(Error range [ER] is $\pm 2\%$).

TABLE 3. Surface roughness and weight change

Sintering Method	TiO ₂ Wt.%	Porosity (μm)			Weight (g)		Weight (g) Change
		Ra	Rz	Rq	Before Wear Test	After Wear Test	
Furnace	3	2.88	16.78	3.49	2.004	2.001	-0.15
Furnace	9	2.58	20.62	3.32	2.016	2.012	-0.21
Furnace	15	2.91	19.47	3.58	2.007	1.994	-0.63
Induction	3	2.89	18.9	3.5	2.016	2.021	0.27
Induction	9	2.68	20.3	3.33	2.013	2.03	0.85
Induction	15	2.25	17.21	2.8	2.017	2.045	1.37

^a(Error range [ER] is $\pm 2\%$).

hardness measurement apparatus at a load of 60 N using a steel ball of 2.5 mm diameter. The Surface roughness test was made using a Mitutoyo Surf SJ-301 profilometer. To understand the relation between surface roughnesses and wear test results (friction coefficient, weight change) we chose the samples with 3, 9 and 15 wt.% TiO₂ reinforcement because they show the maximum effect (Table 3). After cutting the specimens they were hot mounted using a citopress mounting press. The surface of sample was grinded with 200, 400, 600, 800, 1000 and 1200 emery paper. After grinding the surface of sample was polished using a solution with 1 micron particle size of alumina suspension. The images of the microstructure were taken with Meiji Techno Metallurgical Microscope.

3. RESULTS

The influence of TiO₂ reinforcement on density and hardness values are given in Table 1 and 2 for furnace and induction respectively. The influence on wear resistance and porosity are given in Table 3.

It can be seen in Table 1 and 2 induction sintered samples are about 2% harder than the samples sintered in furnace. The hardness of the sample increases for wt. 3% and 5% TiO₂ reinforcement. By increasing the reinforcement it is obvious that the hardness decreases significantly.

Roughness and friction coefficient of porous titanium dioxide films increase with increasing TiO₂ concentration. Generally porosity causes higher roughness values and the coefficient of friction (COF)

increases with increasing roughness according to the literature (Piwoński, 2007). Our observation shows that this is not the case. The roughness does not show the same correlation with COF depending on the amount of reinforcement.

During annealing the diffusion at the interface layer has an effect on mechanical properties of Al-TiO₂ composites. Since Gibbs free energy of formation for Al₂O₃ is lower than that of TiO₂, a short range thermal diffusion of constituent elements can occur at the interface. The annealing time stimulates the decomposition process and induces a large diffused area which results a mixture of Al₂O₃ and Al₃Ti fragments in the aluminium matrix. The decomposition of the particles and their microstructural evolution depends on annealing time and the size of particles as mentioned in literature (Shin *et al.*, 2013). Sintering methods cause difference in mechanical and tribological values, which can be due to the different sintering time and heating rate. At higher heating rate amorphous TiO₂ transformed to rutile directly while at a lower heating rate the TiO₂ phase will be anatase at 500–800 °C. The Mohs scale for rutile is around 6.0–6.5 and for anatase 5.5–6.0. We observed that, induction sintered samples have higher hardness values than furnace sintered samples (Tables 1 and 2).

Increasing the weight percentage of TiO₂ as seen in microstructure images (Figs. 1–4) cause an increase in the grain size and grain boundary region. The porosity between grain boundaries increases with increasing reinforcement. For both sintering methods above 5 wt.% reinforcement the hardness has a tendency to decrease (Figs. 8 and 9).

Addition up to 1 wt.% TiO₂ in tin-lead solders decreases the grain size and width of the grain boundary. The decrease resulted in an increase in hardness. For reinforcement with 2 wt.% TiO₂ microporosity was observed at the grain boundary region. Moreover, increased reinforcement porosity can form microscopic cracks which are detrimental to strength as reported by work (Lin *et al.*, 2003). This is consistent with our observations and explains the sharp fall in hardness values (Figs. 8 and 9) for reinforcement above 9 wt.% TiO₂.

The density change absolute value of green and sintered composites for both sintering methods are given in Fig. 5. Induction sintered samples have a little change in density up to 9 wt.% reinforcement. Furnace sintered specimens density increases linearly but drops after 9 wt.% reinforcement but at the same percent reinforcement the volume increases and hardness decreases sharply (Fig. 7). For both sintering methods volume increases continuously after

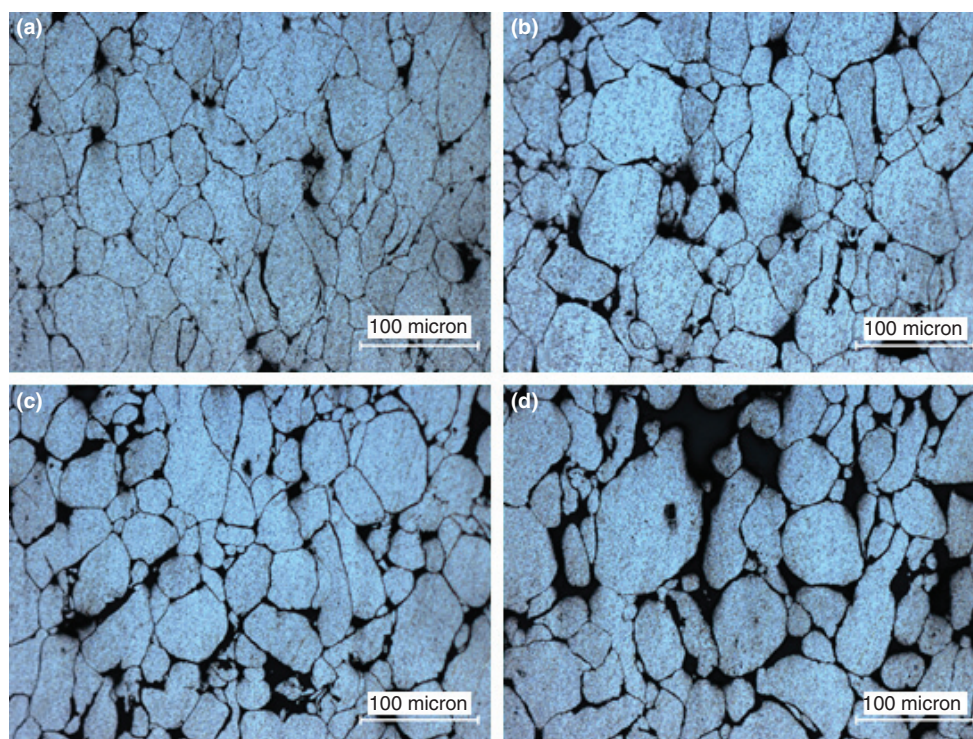


FIGURE 1. The micrographs of furnace sintered samples at 200X zoom: a) 3, b) 5, c) 9 and d) 15 wt. % TiO₂.

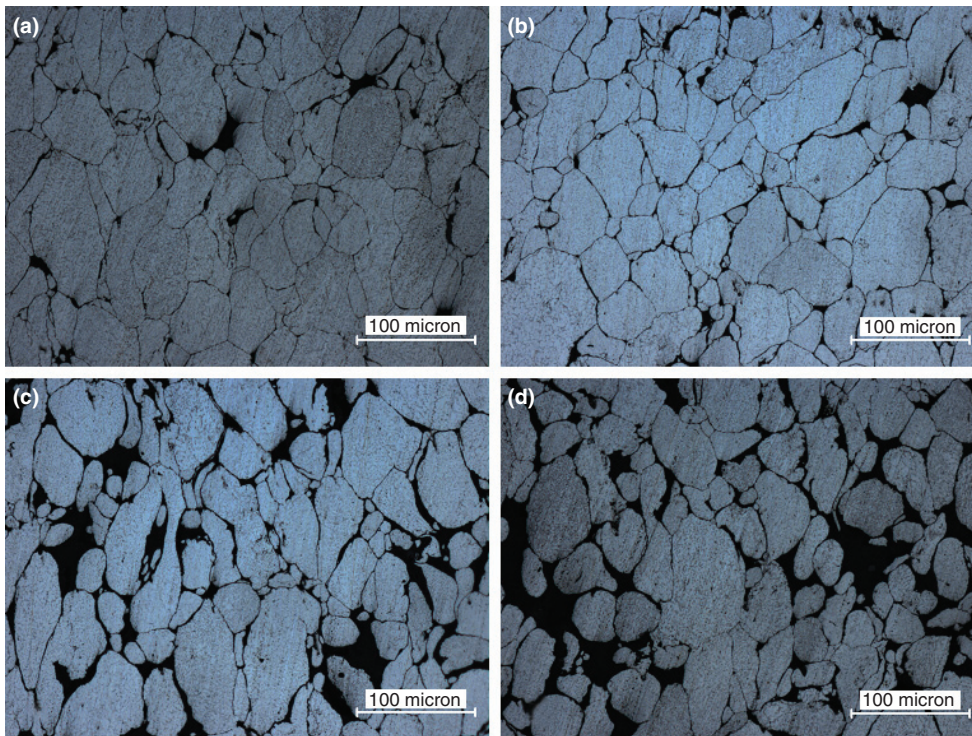


FIGURE 2. The micrographs of induction sintered samples at 200X zoom: a) 3, b) 5, c) 9 and d) 15 wt.% TiO_2 .

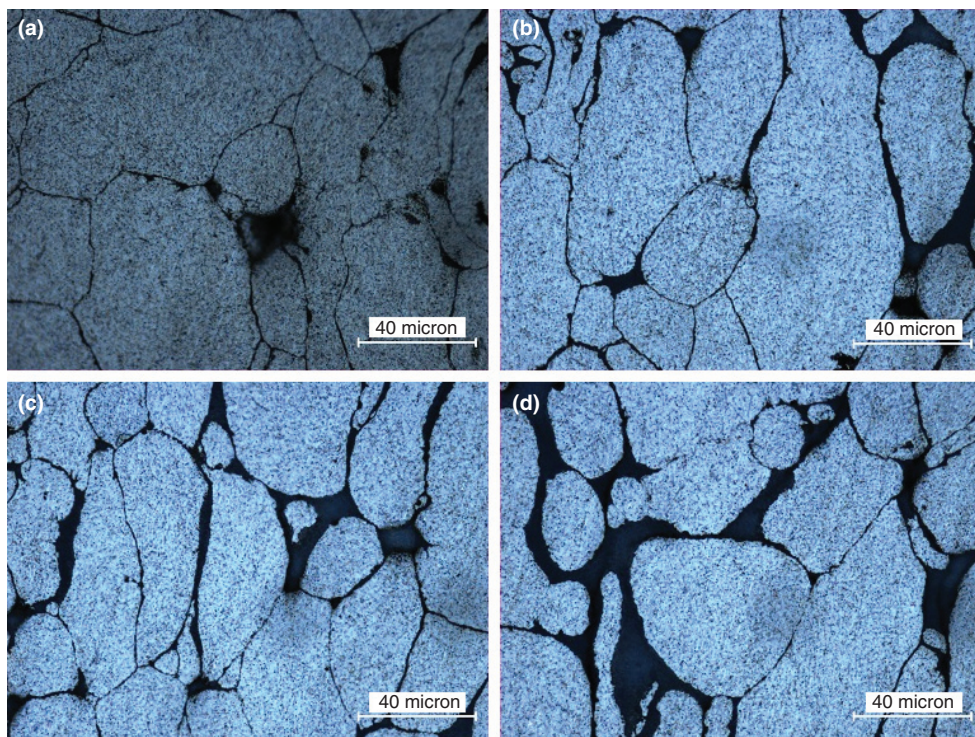


FIGURE 3. The micrographs of furnace sintered samples at 500X zoom: a) 3, b) 5, c) 9 and d) 15% wt. TiO_2 .

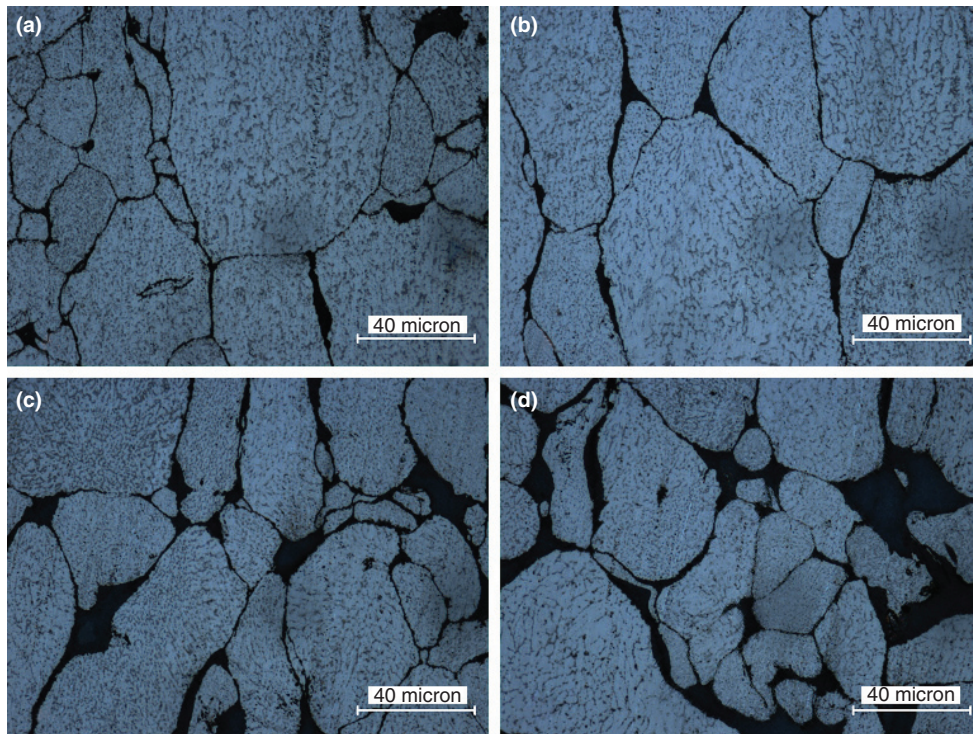


FIGURE 4. The micrographs of induction sintered samples at 500X zoom: a) 3, b) 5, c) 9 and d) 15 %wt. TiO₂.

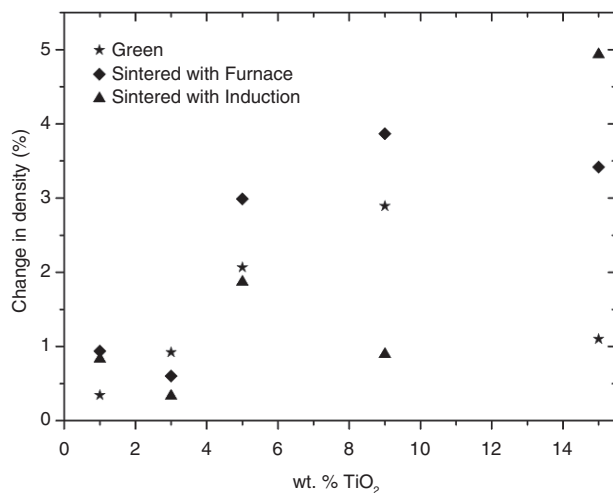


FIGURE 5. The absolute values of density change percent of samples with different reinforcement of TiO₂.

5 wt.% reinforcement (Figs. 6 and 7). The hardness has a maximum value at 5 wt.% and a minimum value at 15 wt.% (Figs. 8 and 9).

At 900 °C sintered Cu-5 wt.% TiO₂ composites have a maximum hardness as mentioned in literature (Sorkhe *et al.*, 2014). We have observed similar results. The hardness results are given in Tables 1–2 and shown in Figs. 8–9. An increase up to 5 wt.% reinforcement cause an increase in hardness. Above 9 wt.% reinforcement causes a sharp decrease in hardness.

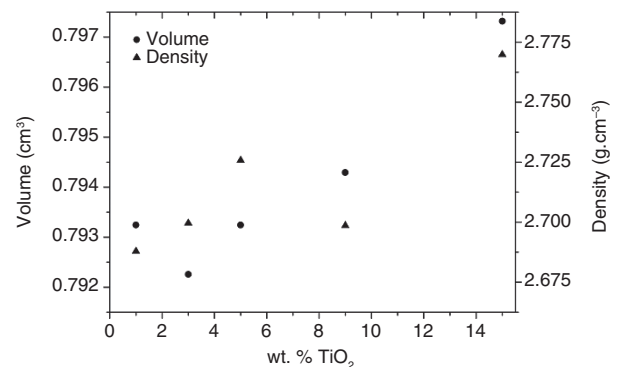


FIGURE 6. Volume and density of induction sintered samples for various amount of reinforcement.

According to literature (Khodabakhshi *et al.*, 2014) annealing time and temperature have different effects on Al-Mg- 3, 5, 6 vol. % TiO₂ like microstructure and mechanical properties. Sintering time has an effect on the chemical reaction between Al and TiO₂. The heating rate and sintering time is quite different for furnace and induction sintering. This difference explains also the wear behavior of samples which are sintered with different methods. At higher heating rate like in induction, the samples are harder. An increase in hardness causes an increase in wear resistance. The weight change (Fig. 10) after wear test (Tables 2 and 3) indicates that counterpart is worn up during wear test.

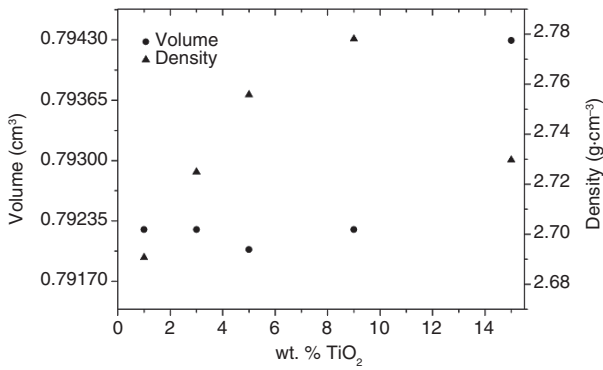


FIGURE 7. Volume and density change of furnace sintered samples for various amount of reinforcement.

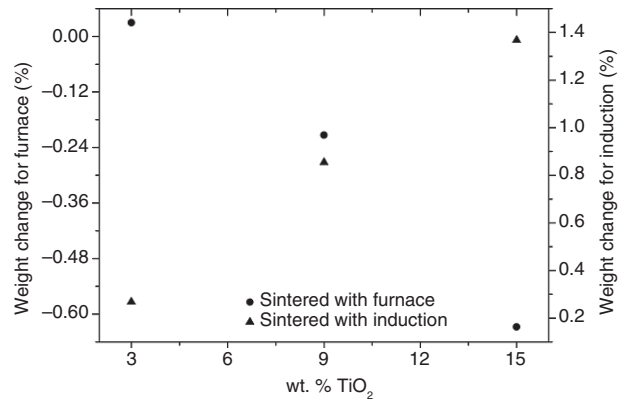


FIGURE 10. Weight change percentage after wear test for various amount of reinforcement.

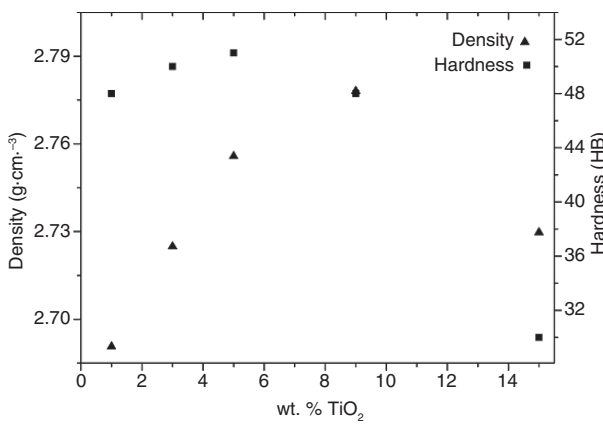


FIGURE 8. Density and hardness of furnace sintered samples for various amount of reinforcement.

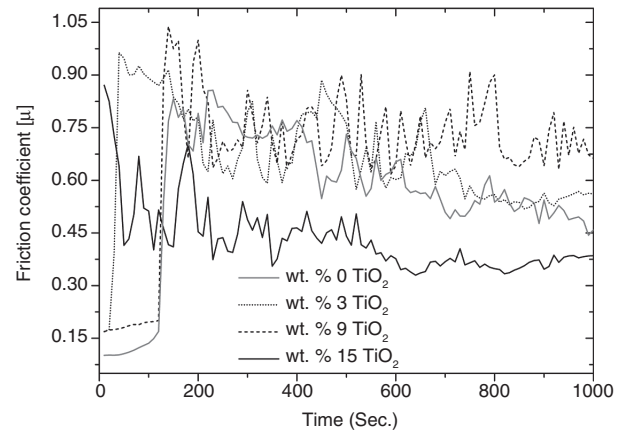


FIGURE 11. Wear test results for induction sintered samples with various amount of reinforcement.

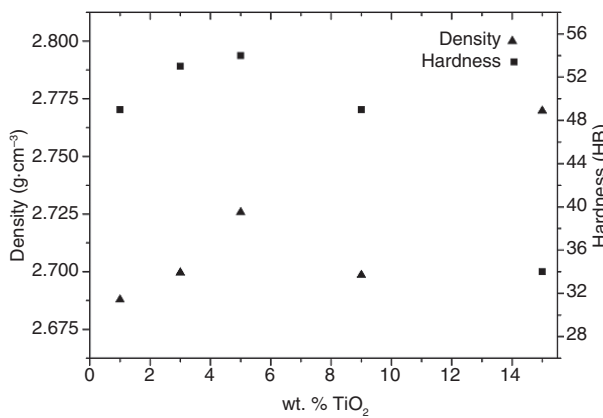


FIGURE 9. Density and hardness of induction sintered samples for various amount of reinforcement.

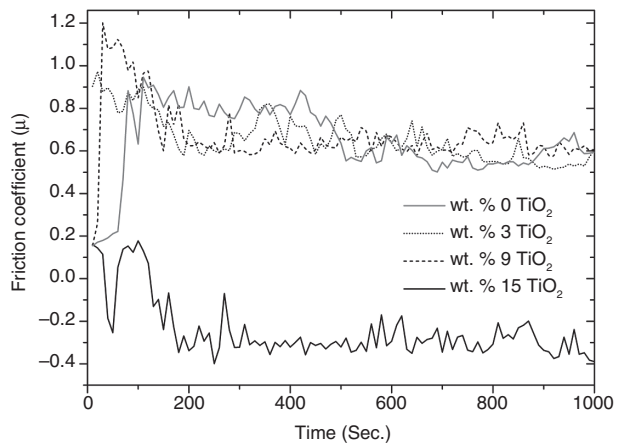


FIGURE 12. Wear test results for furnace sintered samples with various amount of reinforcement.

The wear test results for Al and Al-TiO₂ composites are shown in Figs. 11 and 12. The friction coefficient (COF) of furnace sintered pure Al and 3, 9 wt.% reinforced samples show an increase at the beginning of the first 10 meters of sliding distance and small fluctuations after 50 meters. It shows a negative

drop in COF although reinforcement increased by 15 wt.% (Fig. 12). Negative friction force reported by Chen and Zhau (2003). The reason for this can be the high surface roughness (Table 3) which causes high

TABLE 4. Green density of Al-TiO₂ composites

Wt.% TiO ₂	Weight (g) Before Press	Weight (g) After Press	Density (g·cm ⁻³)
1	2.0375	2.0334	2.6657
3	2.0085	2.0024	2.7086
5	2.0188	2.0157	2.6758
9	2.025	2.0178	2.6747
15	2.0192	2.0163	2.6395

^a(Error range [ER] is $\pm 2\%$).

vibration which can cause sample counterpart contact problems during wear test. In the same time the results show high wear loss (Fig. 10) and less COF (Fig. 12). As seen in Table 3 (Fig. 10) induction sintered samples have a higher wear resistance, higher hardness and a lower density than in furnace sintered samples. Comparing Figs. 3b, 3d and Figs. 4b, 4d it can be concluded that induction sintered samples have a better compaction.

By comparison the friction coefficient of induction sintered samples (Fig. 11) with furnace sintered samples (Fig. 12) we see a good relation for 3 and 9 wt.% of TiO₂. But there is a significant change in COF for 15 wt.% of TiO₂. The weight change (Table 4) after wear test indicates wear loss in counterpart.

The wear test of induction sintered samples show a great fluctuation in COF compared to the samples sintered in furnace. It is obvious that the sintering method and reinforcement amount has a great effect on surface roughness, wear resistance and hardness. In furnace sintered samples have a greater wear loss during wear test (Fig. 10). The furnace sintered samples show a stable friction coefficient of 0.6 μ after 200 seconds of sliding time (Figs. 11 and 12).

Aniolek *et al.* (2016) reported for oxidised titanium surface at 600 °C in the initial stage of wear test a significant increase in the coefficient of friction up to 0.8–0.9 and stabilises at 0.5–0.65. Leng *et al.* (2007) reported in their work very stable friction coefficient about 0.5 after 500 cycles for titanium dioxide deposited Ti6Al4V substrate. The titanium alloy showed an unstable friction coefficient in the range of 0.5–0.8 after 2000 cycles. Also the mass loss was smaller for TiO₂ deposited substrate. Both are a good agreement with our results (Figs. 11–12).

4. CONCLUSIONS

- The green density decrease after 9 wt.% of TiO₂ (Table 4). The density of sintered samples are higher than green density. Also the density of samples with 15 wt.% TiO₂ has a significant difference for different sintering methods.
- The results Show that the mechanical and tribological values are different for induction and

furnace sintering. This is because of the difference in the sintering time and the heating rate.

- It can be concluded that the composites for low reinforcement show slight change in the wear resistance compared to pure aluminium. But reinforcement of wt. 15% TiO₂ decreases the COF by both methods. Porosity has a important effect with increasing reinforcement on the sample.
- The Brinell hardness drops significantly to a minimum value for both sintering methods with wt. 15% TiO₂. The hardness value has a maximum for value wt. 5% TiO₂ for both sintering methods.
- The microstructure images show that the particle bonds decreases and the porosity increases with increasing reinforcement. This has a great effect on hardness and wear resistance.
- For the application Al-TiO₂ composite in industries, furnace and induction sintering parameters is optimized. With a proper fabrication process, relatively high density and high dispersion degrees of dispersion of TiO₂ nanoparticles are achieved. The strength of the composite increases with increasing volume contents up to 5 wt.% TiO₂ nanoparticle reinforcement. It suggests that the 1–5 wt.% TiO₂ reinforcement and induction sintering as fabrication processes with less time and less energy are suitable for successful composite preparation. These results may open new perspectives for the applications of such composites as structural components.

ACKNOWLEDGMENT

This work was supported by Celal Bayar University Scientific and Research Commission under the Project number 2015-010.

REFERENCES

- Aniolek, K., Kupka, M., Barylski, A. (2016). Sliding wear resistance of oxide layers formed on a titanium surface during thermal oxidation. *Wear* 356–357, 23–29. <https://doi.org/10.1016/j.wear.2016.03.007>.
- Chen, G.X., Zhau, Z.R. (2003). Correlation of a negative friction-velocity slope with sequal generation under reciprocating conditions. *Wear* 255, 376–384.
- Chuang, L.-C., Luo, C.-H., Yang, S.-H. (2011). The structure and mechanical properties of thick rutile-TiO₂ films using different coating treatments. *Appl. Surf. Sci.* 258 (1), 297–303. <https://doi.org/10.1016/j.apsusc.2011.08.055>.
- Çavdar, U., Gülşahin, İ. (2014). Ultra high frequency induction welding of powder metal compact. *Rev. Metal.* 50 (2), e016. <https://doi.org/10.3989/revmetalm.016>.
- Çavdar, P.S., Çavdar, U. (2015). The evaluation of different environments in ultra-high frequency induction sintered powder metal compacts. *Rev. Metal.* 51 (1), e036. <https://doi.org/10.3989/revmetalm.036>.
- Gökçe, A., Fındık, F. (2008). Mechanical and physical properties of sintered aluminum powders. *J. Achiev. Mater. Manuf. Eng. (JAMME)* 30 (2), 157–164. <https://citeseerx.ist.psu.edu/viewdoc/download?doi=10.1.1.563.1942&rep=rep1&type=pdf>.

- Hassani, A., Bagherpour, E., Qods, F. (2014). Influence of pores on workability of porous Al/SiC composites fabricated through powder metallurgy mechanical alloying. *J. Alloy. Compd.* 591, 132–142. <https://doi.org/10.1016/j.jallcom.2013.12.205>.
- Khodabakhshi, F., Simchi, A., Kokabi, A.K., Gerlich, A.P., Nosko, M. (2014). Effects of post-annealing on the microstructure and mechanical properties of friction stir processed Al-Mg-TiO₂ nanocomposites. *Mater. Design* 63, 30–41. <https://doi.org/10.1016/j.matdes.2014.05.065>.
- Leng, Y.X., Chen, J.Y., Yang, P., Sun, H., Huang, N. (2007). The microstructure and properties of titanium dioxide films synthesized by unbalanced magnetron sputtering. *Nucl. Instrum. Meth. B* 257 (1–2), 451–454. <https://doi.org/10.1016/j.nimb.2007.01.096>.
- Li, D., Chen, S., Wang, D., Li, Y., Shao, W., Long, Y., Liu, Z., Ringer, S.P. (2010). Thermo-analysis of nanocrystalline TiO₂ ceramics during the whole sintering process using differential scanning calorimetry. *Ceram. Int.* 36 (2), 827–829. <https://doi.org/10.1016/j.ceramint.2009.10.004>.
- Lin, D.C., Wang, G.X., Srivatsan, T.S., Al-Hajri, M., Petraro, M. (2003). Influence of titanium dioxide nanopowder addition on microstructural development and hardness of tin-lead solder. *Mater. Lett.* 57 (21), 3193–3198. [https://doi.org/10.1016/S0167-577X\(03\)00023-5](https://doi.org/10.1016/S0167-577X(03)00023-5).
- Lumley, R. (2011). *Fundamentals of Aluminium Metallurgy: Production, Processing and applications*. 1st Edition, Woodhead Publishing Limited, p. 678.
- Mazaheri, M., Zahedi, A.M., Haghigatzadeh, M., Sadrnezhad, S.K. (2009). Sintering of titania nanoceramic: Densification and grain growth. *Ceram. Int.* 35 (2), 685–691. <https://doi.org/10.1016/j.ceramint.2008.02.005>.
- Pinto, D., Bernardo, L., Amaro, A., Lopes, S. (2015). Mechanical properties of epoxy nanocomposites using titanium dioxide as reinforcement – A review. *Constr. Build. Mater.* 95, 506–524. <https://doi.org/10.1016/j.conbuildmat.2015.07.124>.
- Piwoński, I. (2007). Preparation method and some tribological properties of porous titanium dioxide layers. *Thin Solid Films* 515 (7–8), 3499–3506. <https://doi.org/10.1016/j.tsf.2006.10.115>.
- Pydi, H.P.R., Adhithan, B., Bakrudeen, A.S.B. (2013). Microstructure Exploration of the Aluminum-Tungsten Carbide Composite with different Manufacturing circumstances. *IJSCE* 2 (6), 257–261.
- Raut, A., Choudhary, D. (2015). Nano enabled coatings makes aircraft invisible. *Int. J. Pure Appl. Res. Eng. Techn. (IJPRET)* 3 (9), 134–146. <http://www.ijpret.com/publishedarticle/2015/4/IJPRET%20-%20MECH%20127.pdf>.
- Shin, J.H., Choi, H.J., Bae, D.H. (2013). Evolution of the interfacial layer and its effect on mechanical properties in TiO₂ nanoparticle reinforced aluminium matrix composites. *Mat. Sci. Eng. A-Struct.* 578, 80–89. <https://doi.org/10.1016/j.msea.2013.04.069>.
- Singh, M., Goyal, K., Goyal, D.K. (2015). Fabrication performance of aluminium based metal matrix composites with SiO₂ and TiO₂ as reinforced particles. *Universal J. Mech. Eng.* 3 (4), 142–146. <https://doi.org/10.13189/ujme.2015.030404>.
- Sorkhe, Y.A., Aghajani, H., Tabrizi, A.T. (2014). Mechanical alloying and sintering of nanostructured TiO₂ reinforced copper composite and its characterization. *Mater. Design* 58, 168–174. <https://doi.org/10.1016/j.matdes.2014.01.040>.
- Tubio, C.R., Guitián, F., Salguero, J.R., Gil, A. (2015). Anatase and rutile TiO₂ monodisperse microspheres by rapid thermal annealing: A method to avoid sintering at high temperatures. *Mater. Lett.* 141, 203–206. <https://doi.org/10.1016/j.matlet.2014.11.063>.
- Xiang, N., Song, R., Zhao, J., Li, H., Wang, C., Wang, Z. (2015). Microstructure and mechanical properties of ceramic coatings formed on 6063 aluminium alloy by micro-arc oxidation. *T. Nonferr. Metal. Soc.* 25 (10), 3323–3328. [https://doi.org/10.1016/S1003-6326\(15\)63988-7](https://doi.org/10.1016/S1003-6326(15)63988-7).